ELSEVIER

Journal of Nuclear Materials 258–263 (1998) 706–712

journal of nuclear materials

# Development of multi-element doped graphite and its modification of chemical erosion

J.P. Qian [a,*], J. Roth [b], J.R. Song [a], F. Zhang [a], L. Yang [a], G.T. Zhai [a]

[a] *Southwestern Institute of Physics, P.O. Box 432, Sichuan 610041, People's Republic of China*
[b] *Max-Planck Institute for Plasma Physics, EURATOM Association, D-85748 Garching, Germany*

**Abstract**

A series of B-, Ti- and Si-doped graphite has been recently developed in China as low-$Z$ plasma facing materials (PFMs) for reducing the chemical sputtering (CS) and radiation enhanced sublimation (RES). The erosion experiment indicates that the CS yield of doped graphite at 1 keV and 50 eV $D^+$ bombardment was decreased by factor of 5 and 20–30%, respectively, in comparison with that of pure graphite. Raman spectrum analysis and scanning electron microscope (SEM) observation showed that the doped graphite was more stable under $H^+$ bombardment. 

## 1. Introduction

Graphite and other carbon base materials have been used as low-$Z$ (atomic number) plasma facing materials (PFMs) in fusion plasma experimental devices for a long time and they were very attractive because of their good thermo-physical properties. Unfortunately, graphite is heavily eroded by hydrogen ions due to chemical sputtering (CS) in the temperature range between room temperature (RT) and 800°C and due to radiation enhanced sublimation (RES) at temperatures above 1000°C, which is frequently exceeded in present large tokamaks and reactor design. High carbon erosion limits the component lifetime and can lead to excessive plasma contamination. On the other hand, beryllium was found to be a good low-$Z$ PFM for many large tokamaks since the plasma parameters in those tokamaks where Be was used as PFM were improved obviously. Be is now considered as a primary candidate for the first wall material in ITER [1]. Due to the fact that carbon does not melt even at very high transient heat loads carbon base materials are still the choice for the divetor plate material and protection limiters in the main vessel. Some B-, Ti- and Si-doped graphites were developed for suppressing CS and RES at elevated temperature and they were, in fact, a kind of ceramic (e.g. $B_4C$, TiC and SiC) doped/mixed graphite [2–7]. The experimental results show that the CS is reduced and RES is shifted to higher temperatures in ion beam erosion experiments.

## 2. Experimental

A series of B-, Ti- and Si-doped graphites has been developed in China recently. There were five kinds of doped graphites in the series: (1) B-doped graphite, (2) Ti-doped graphite, (3) B- and Ti-doped graphite, (4) B- and Si-doped graphite, (5) B-, Ti- and Si-doped graphite. The former two kinds of doped graphite have been tested in many laboratories in the world and they will not be discussed in this paper. Overall, B doping was very effective in reducing the CS [8], while addition of Ti increased the thermal conductivity [9]. The idea of doping two or three elements into the graphite was to get low CS and high thermal conductivity in these doped graphite. Their thermal conductivity was measured at room temperature.

The CS experiments were performed in an erosion test apparatus which was equipped with mass analysed high current deuterium ion source, a vaccum microbalance and a quadrupole mass spectrometer (QMS) [10].

* Corresponding author. Tel.: +86 10 6205 6623; fax: +86 10 6202 1601; e-mail: jpqian@public.east.cn.net.

0022-3115/98/$19.00 
PII: S0022-3115(98)00376-6

Table 1
Thermo-physical parameters of doubly and triply doped-graphites

| Material type | Specimen number for CS | Content of dopants (wt%) | | | Density (g/cm$^3$) | Porosity (%) | Bend strength (MPa) | Thermal expansion coefficient ($10^{-6}$/K) | Thermal conductivity (W/m K) |
|---|---|---|---|---|---|---|---|---|---|
| | | $B_4C$ | Ti | Si | | | | | |
| G-5 | 1# | 0 | 0 | 0 | 1.83 | <10 | 34.2 | | 72.0 |
| GBS-105 | 2# | 10 | 0 | 5 | 2.10 | 4.70 | 102.9 | 3.06 | 39.6 |
| GBT-78 | | 7 | 8 | 0 | 2.13 | 5.70 | 74.3 | 3.38 | 71.65 |
| GBT-105 | | 10 | 5 | 0 | 2.17 | 4.05 | 88.4 | 3.33 | 67.75 |
| GBT-155 | | 15 | 5 | 0 | 2.12 | 5.23 | 90.9 | | 75.30 |
| GBT-205 | | 20 | 5 | 0 | 2.09 | 6.34 | 104.1 | 4.78 | 71.25 |
| GBTS-863 | | 6.5 | 8.5 | 3 | 2.14 | 5.92 | | 4.63 | 68.50 |
| GBTS-864 | 3# | 8 | 6 | 4 | 2.17 | 4.93 | 123.3 | 2.96 | 59.40 |
| GBTS-872 | | 8.2 | 7.7 | 2.5 | 2.03 | 8.54 | | 3.31 | 60.85 |
| GBTS-941 | 4# | 9 | 4.8 | 1.6 | 2.12 | 5.33 | | | 68.40 |

The doped graphite specimen, as an ion beam target, was mounted on a holder and could be heated up to 1200 K by electron bombardment from the rear. The temperature of the specimen could be measured with an infrared pyrometer. The target was surrounded by a double cylinder. The outer one was biased at −50 V to suppress the secondary electrons emitted from beam defining apertures located at the entrance of the target chamber, while the inner one was at ground potential. The deuteron beam from the ion source was decelerated between the inner cylinder and the target biased at positive potential. In the present experiment the ion beam energy of bombarding the target was 1000 and 50 eV, respectively. The current on the target and the inner cylinder could be measured separately and were added for proper charge collection. The reaction products generated on the target during ion beam bombardment were analyzed with a Balzers 511 QMS which was separated from the target chamber by a tube aperture and surrounded by a liquid nitrogen cooled shield [10].

## 3. Results and discussion

Thermo-physical parameters of the two and three dopant mixed graphites recently developed in China are given in Table 1, where G-5 is the pure graphite for comparison. The B- and Si-doped graphite, GBS-105, has high bend strength but its thermal conductivity is too low. The highest bend strength among four types of B- and Ti-doped graphite was reached in GBT-205 while the highest thermal conductivity was reached in GBT-155. Concerning the B-, Ti- and Si-doped graphites, they have an average thermal conductivity and higher bend strength. The influences of the dopant content on the strength and thermal conductivity in two and three element doped graphites is complex. Boron atoms which replace the carbon atoms in the crystal lattice may decrease the thermal conductivity of the B-solved graphite. However, the solubility of boron in carbon materials is very limited, smaller than 2%, such that the second phase of ceramic carbide should exist in the doped graphite. $B_4C$ may catalyze the graphization of carbon and has the active effect on the increasing thermal conductivity in some case. Adding titanium is believed to enhance the thermal conductivity, but adding Si- into the B-doped graphite seems to decrease the thermal conductivity further.

GBS-105, GBT-864 and GBTS-941 have been selected as specimen materials for CS experiments and they were cut into small pieces, which were numbered 2#, 3# and 4#, respectively, while pure graphite (specimen number 1#) was also selected for comparison. The dominant CS product was methane ($CD_4$)under both 1 keV and 50 eV bombard energy and signal of $CD_4$ was collected by the QMS. The QMS signal vs. specimen

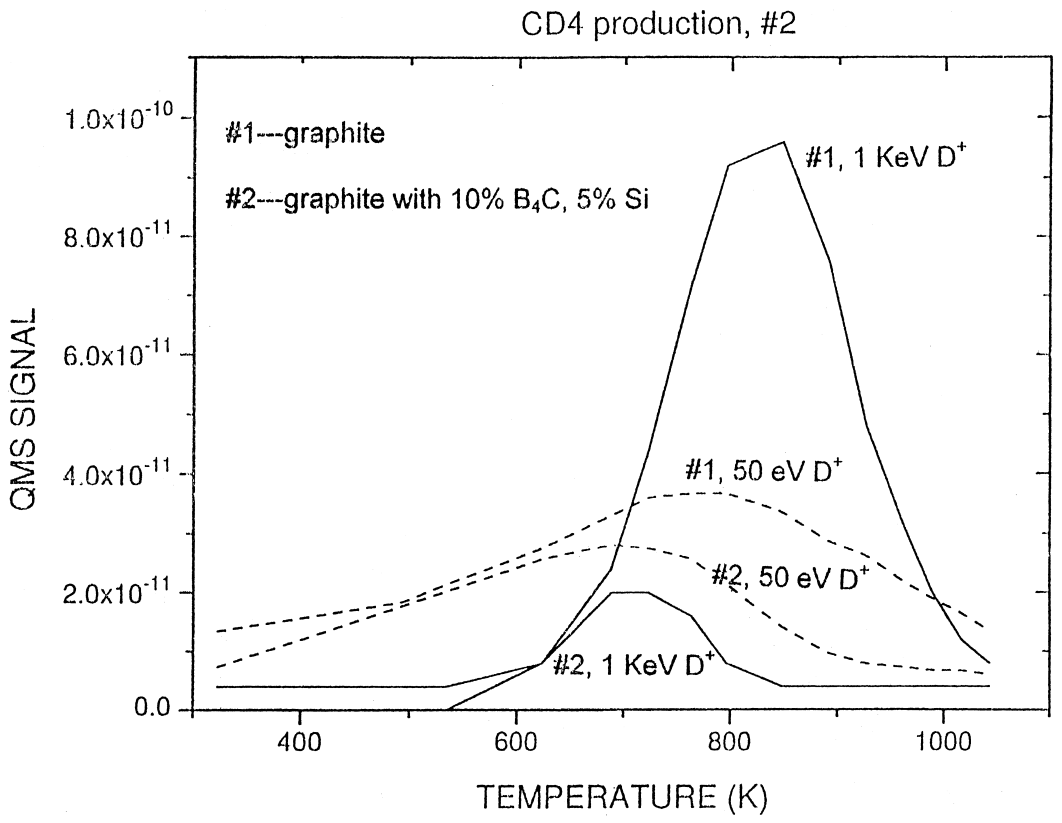


Fig. 1. CS of graphite and B- and Si-doped graphite under 1 keV and 50 eV $D^+$ bombardment (specimen #2).

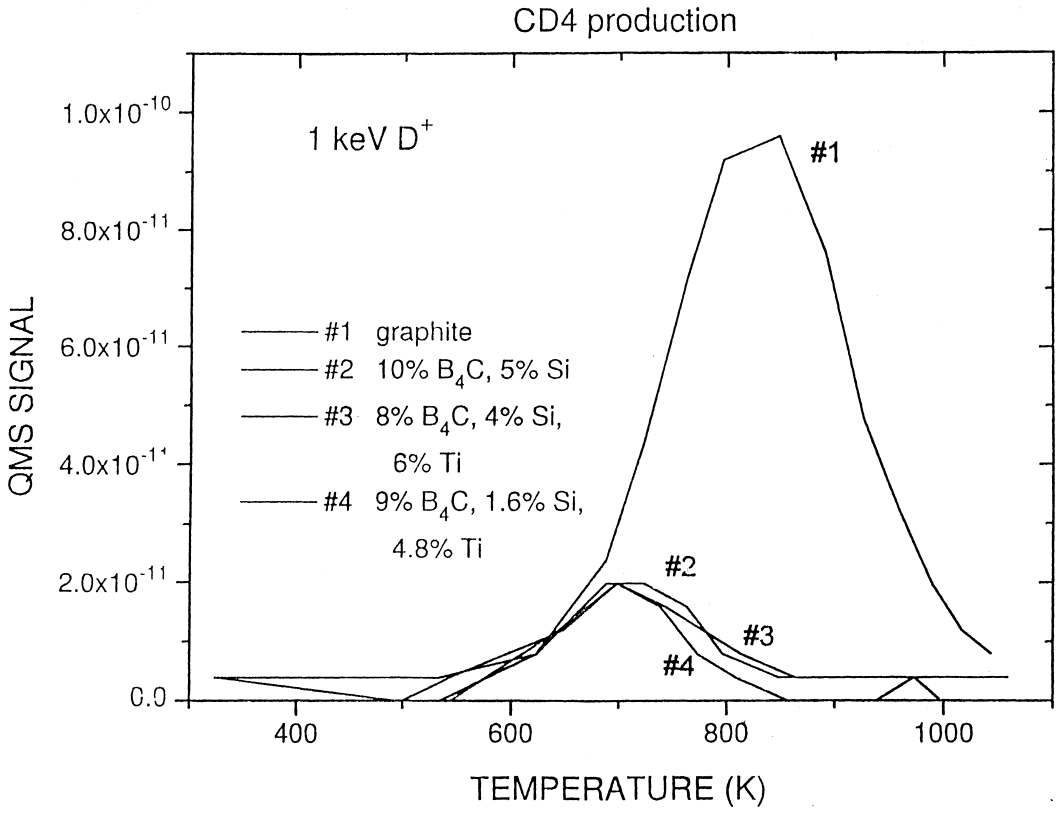


Fig. 2. CS of graphite and three kinds of B-, Si- and Ti-doped graphite under 1 keV $D^+$ bombardment.

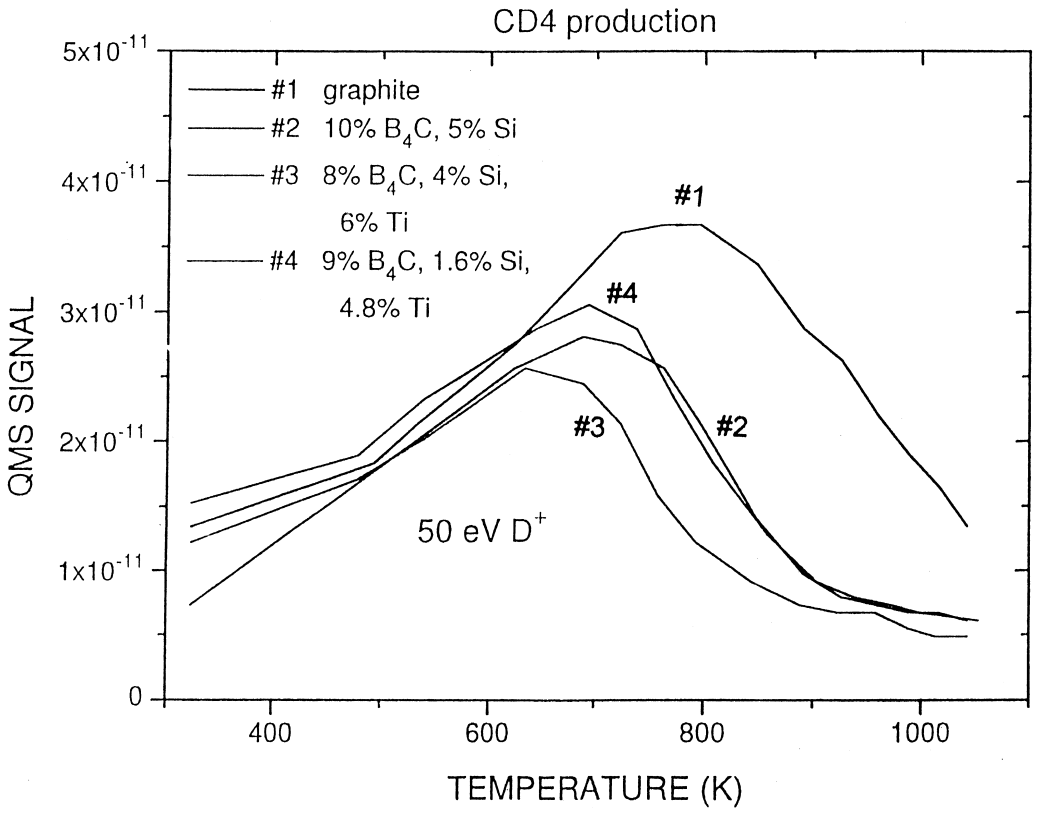


Fig. 3. CS of graphite and three kinds of B-, Si- and Ti-doped graphite under 50 eV $D^+$ bombardment.

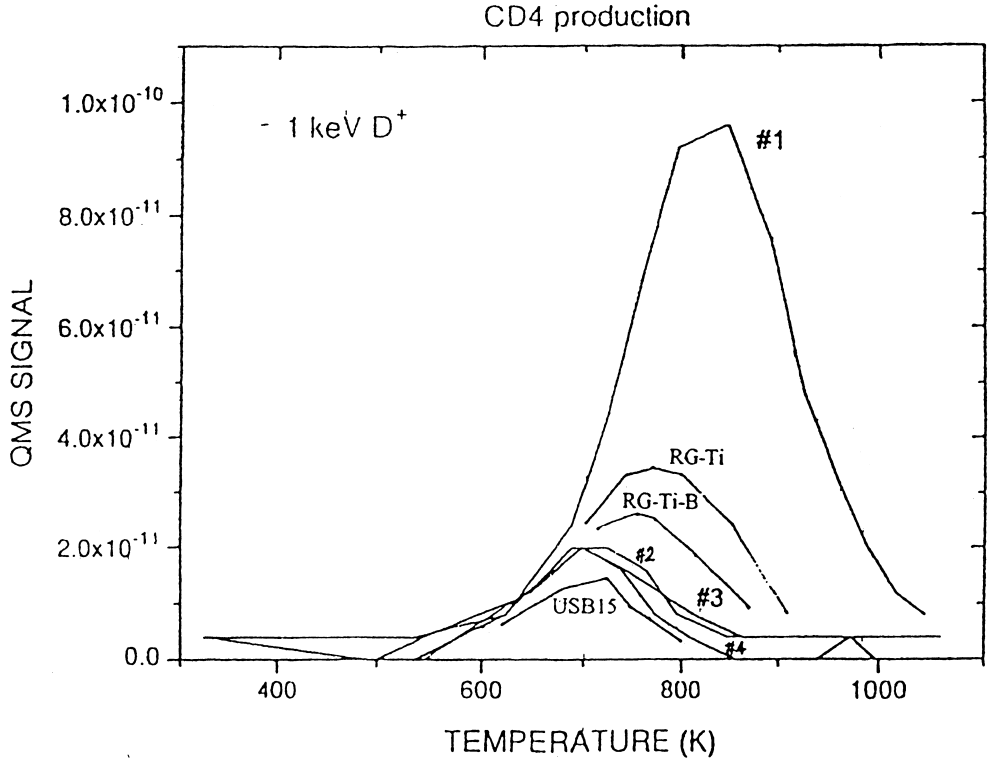


Fig. 4. CS of four kinds of graphite and RG-Ti, RG-Ti–B and USB15 graphite under 1 keV $D^+$ bombardment.

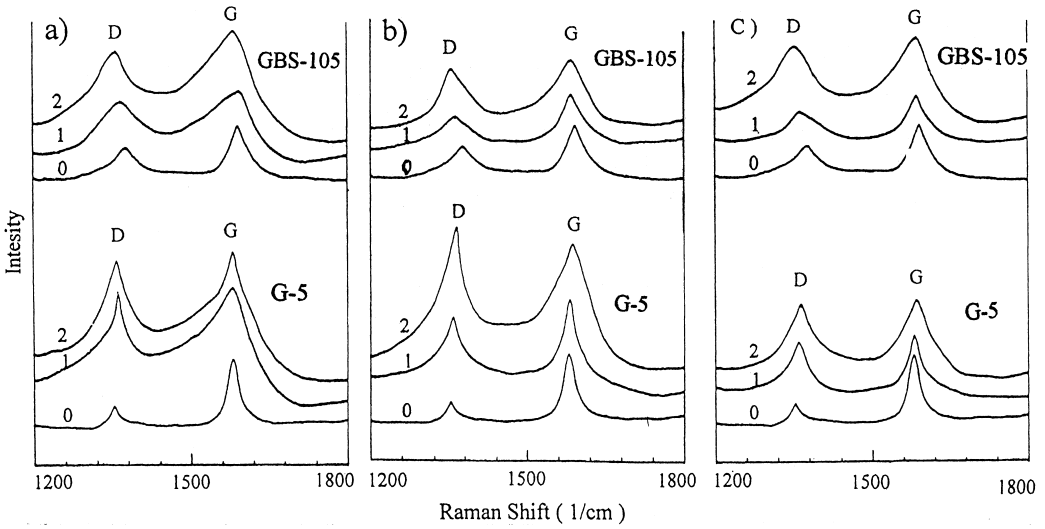


Fig. 5. Raman spectra of G-5 and GBS-105 graphites before and after $H^+$ irradiation: (a) $H^+$ energy 400 eV, specimen temperature RT; (b) $H^+$ energy 400 eV, specimen temperature 550°C; (c) $H^+$ energy 200 eV, specimen temperature RT. 0 – before irradiation, 1 – irradiation dose $8.5 \times 10^{16}$ ions $cm^{-2}$, 2 – irradiation dose $8.5 \times 10^{17}$ ions $cm^{-2}$.

temperature under 1 keV and 50 eV $D^+$ bombardment for specimen 2# is shown in Fig. 1. The CS yield of pure graphite (specimen 1#) is also shown in the figure for comparison. There were also similar curves for specimens 3# and 4#, respectively, but they were omitted to show here. When 1 keV $D^+$ was incident on the graphite and doped graphite specimens, the CS peaks of the three doped graphites were similar and their peak intensities were the same, just equal to 1/5 of CS peak for pure graphite. However, their location shifted towards lower temperatures, the shifts between graphite and the doped graphites being about 110–130 K. In this case the CS has been suppressed effectively. When the energy of the incident $D^+$ beam was decreased to 50 eV, the CS peaks were broadened for both graphite and doped graphite and the maximum yields of doped graphite decreased by 23, 30 and 19% for specimen 2#, 3# and 4#, respectively, in comparison with that of pure graphite (specimen 1#). The CS curves under 1 keV and 50 eV are summarized in Figs. 2 and 3, respectively. The CS curves of doped graphite under 1 keV $D^+$ were almost same while the CS curves under 50 eV showed small differences. The different efficiencies for reduction of the CS yield at 1 keV and 50 eV has been observed earlier for B- doped graphites [5] and was attributed to different erosion processes dominating at different ion energies [11]. While at 1 keV the maximum yield at 580°C is due to the thermal desorption of volatile hydrocarbons the yield for 50 eV at lower temperatures was attributed to ion induced desorption of surface near hydrocarbon radicals. CS yield of GBS-105, GBT-864 and GBTS-941 were compared with that of RG-Ti, RG-Ti–B and USB15 in Fig. 4 [12]. It can be seen that the CS yield of the multiply doped graphite developed in China are lower than that of RG-Ti and RG-Ti–B but a little higher than that of USB15.

The better CS resistance of multi-element doped graphite may be related to its microstructure. Three types of high purity graphite and one doped graphite

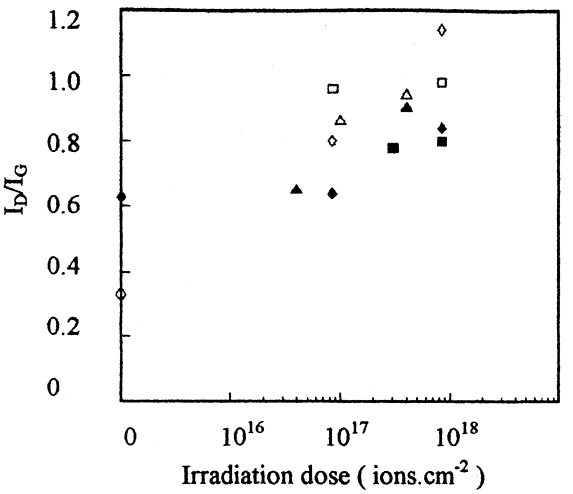


Fig. 6. $I_D/I_G$ vs. irradiation dose of G-5 and GBS-105 graphites under different conditions. The symbols in the figure are: (♦) GBS-105, 400 eV, 550°C; (■) GBS-105, 400 eV, RT; (▲) GBS-105, 200 eV, RT; (●) GBS-105, before irradiation; (◇) G-5,400 eV, 550°C; (□) G-5, 400 eV, RT; (△) G-5,200 eV, RT; (○) G-5, before irradiaton.

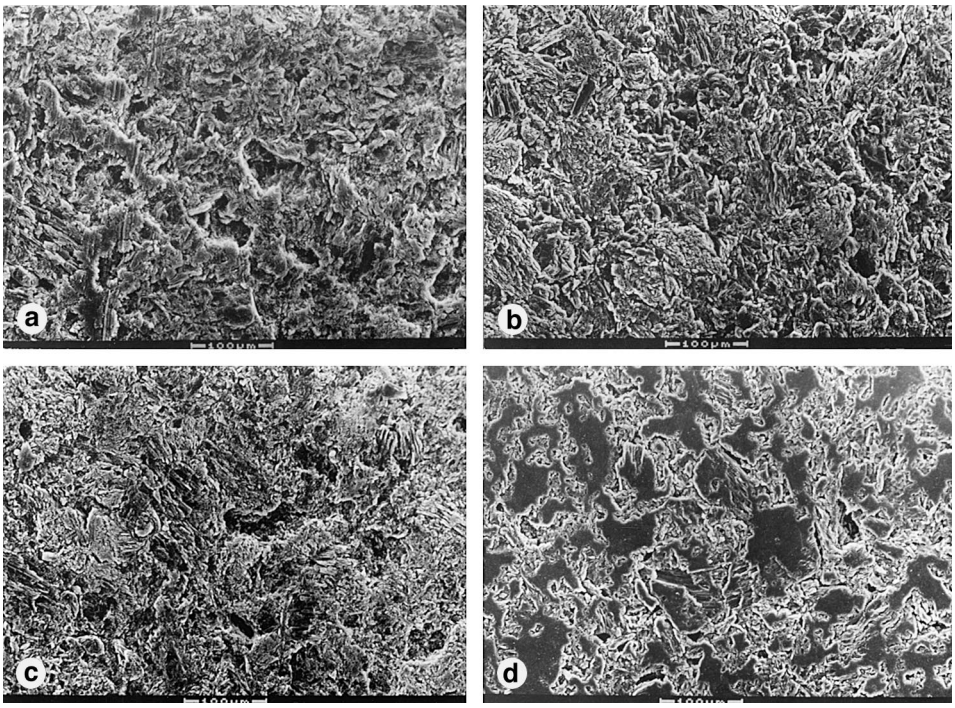


Fig. 7. SEM micrographs of G-5 and GBS-105 graphite before and after 400 eV $H^+$ irradiation.(a) GBS-105, before irradiation; (b) GBS-105, irradiation dose $8.5 \times 10^{17}$ ions $cm^{-2}$, temperature 550°C; (c) G-5, before irradiation; (d) G-5, irradiation dose $8.5 \times 10^{17}$ ions $cm^{-2}$, temperature 550°C.

were analyzed before and after hydrogen ion irradiation using Raman spectrometry (RS). The three pure graphites tested in the experiment were ISO880U (made in Japan), G-5 and T901 (made in China) while the doped graphite was GBS-105. The behaviour of ISO880U, T901 and G-5 was similar both, before and after $H^+$ bombardment. There were two peaks in the Raman spectrum: peak G (1580 $cm^{-1}$) corresponding to the $sp^2$ hybrid bond of carbon atoms in the graphite crystal and the peak D (1355 $cm^{-1}$) corresponding to the $sp^3$ hybrid bond in the graphite. The peak D is also related to defects in the graphite, such that the ratio of $I_D/I_G$ can indicate the completeness of the graphite crystal, where $I_D$ and $I_G$ are the intensities of the peak D and G, respectively. Fig. 5 shows the Raman spectrum of G-5 and GBS-105 before and after $H^+$ irradiation while the ratio of $I_D/I_G$ deduced from Fig. 5 vs. irradiation dose is given in Fig. 6. $I_D/I_G$ of G-5 and GBS-105 before irradiation were ~0.3 and ~0.6, respectively, (see Figs. 5 and 6) indicating that more defects existed in GBS-105 due to the addition of dopants in comparison with that of G-5. But after irradiation, $I_D/I_G$ of G-5 increased sharply with the irradiation dose, up to a value ~1 at the highest dose, while $I_D/I_G$ of GBS-105 only increased slightly with the irradiation dose reaching values around 0.8. So it is obvious that more defects would arise in the pure graphite after $H^+$ irradiation while only few additional defects due to $H^+$ irradiation are produced in doped graphite. These results are consistent with that obtained at other laboratory [12]. The doped graphite seems more stable under hydrogen ion beam radiation. The surface morphology of irradiated G-5 and GBS-105 specimens is shown in Fig. 7. It can be seen in these SEM micrographs that G-5 was eroded heavily after $H^+$ irradiation in the temperature range of CS, e.g. 550°C, while the surface of GBS-105 specimen showed no obvious erosion after irradiation at the same dose and temperature.

## 4. Conclusion

A series of doped graphites has been developed in China for modification of strength, thermal conductivity and CS. Up to now only three kinds of doped graphite have been tested and the results obtained from these three doped graphites are presented. CS of the doped graphites was decreased by a factor of 5 under 1 keV $D^+$ bombardment while under 50 eV $D^+$ irradiation CS was only decreased by 20–30%. CS peak shifts of 110–130 K for doped graphite towards lower temperatures have also been observed in the experiments. The difference between doubly and triply doped graphites is not obvious in CS. Raman spectrum measurements showed

that much less additional defects appeared in doped graphites after $H^+$ irradiation in comparison with pure graphites. The strength of doped graphites has been increased obviously, while the thermal conductivity of B- and Ti-doped graphites was only slightly increased. Thermal conductivity of B-, Ti- and Si-doped graphite was similar in comparison with that of pure graphite. The experimental investigations on the series of doped graphite has not yet been finished and further experiments are required.

## References

[1] R. Parker et al., J. Nucl. Mater. 241–243 (1997) 1.
[2] Y. Hirooka et al., J. Nucl. Mater. 176&177 (1990) 473.
[3] E. Vietzke et al., J. Nucl. Mater. 176&177 (1990) 481.
[4] T. Hino, T. Yamashina, J. Nucl. Mater. 196–198 (1992) 531.
[5] C. Garcia-Rosales, J. Roth, J. Nucl. Mater. 196–198 (1992) 573.
[6] C. Garcia-Rosales et al., J. Nucl. Mater. 189 (1992) 1.
[7] C. Garcia-Rosales et al., J. Nucl. Mater. 212–215 (1994) 1211.
[8] R. Schwoeer, J. Roth, J. Appl. Phys. 77 (1995) 3812.
[9] T.A. Burtseva et al., J. Nucl. Mater. 191–194 (1992) 309.
[10] W. Eckstein, C. Garcia-Rosales, J. Roth, W. Ottenberger, Max-Planck-Institut fur Plasmaphysik, Report IPP 9/82 (1993).
[11] J. Roth, C. Garcia-Rosales, Nucl. Fusion 36 (1996) 1647; Nucl. Fusion 37 (1997) 897.
[12] K. Niwase et al., J. Nucl. Mater. 179–181 (1991) 214.